Using Distribution of Relaxation Times to Study Proton Exchange Membrane Fuel Cell Stack Ageing

Laurine Turpin
IFP Energies nouvelles
Rond-point de l'échangeur de Solaize, BP 3, 69360 Solaize, France
laurine.turpin@ifpen.fr

Quentin Cacciuttolo
IFP Energies nouvelles
Rond-point de l'échangeur de Solaize, BP 3, 69360 Solaize, France
quentin.cacciuttolo@ifpen.fr

Zhixue Zheng
Université Marie et Louis Pasteur, CNRS, institut FEMTO-ST, FCLAB, F-90000, Belfort, France
zhixue.zheng@umlp.fr

Boyang Xu
IFP Energies nouvelles
1 et 4 avenue de Bois-Préau, 92852 Rueil-Malmaison, France
boyang.xu@ifpen.fr

Marie-Cécile Péra
Université Marie et Louis Pasteur, CNRS, institut FEMTO-ST, FCLAB, F-90000, Belfort, France
marie-cecile.pera@umlp.fr

***Abstract*— This study utilizes the Electrochemical Impedance Spectroscopy (EIS) and the Distribution of Relaxation Times (DRT) to analyse the aging of Proton Exchange Membrane Fuel Cells (PEMFCs). The EIS and DRT are applied on an industrial stack made for transportation application. This study then looks at the relevancy of using DRT on a real-life application and how the scale effect affects the interpretation of the phenomena inside the short stack. The data are generated through an original ageing campaign in the laboratory, and the evolution of DRT across time is studied. Finally, the DRT interpretation for Equivalent Circuit Modelling (ECM) improvement is shown.**

Keywords*— *PEMFC, Ageing, Electrochemical Impedance Spectroscopy, Distribution of Relaxation Times

I. Introduction

Hydrogen systems are highly promising devices to store energy. In particular, Fuel Cells (FC) are presented as a key technology to enhance the sustainable energy transition, when fed with decarbonized dihydrogen.

Due to their compacity, high-power density and low temperature, Proton Exchange Membrane Fuel Cells (PEMFCs) can be interesting for heavy-duty vehicle electrification. Among the challenges that remain to develop the commercialization of this technology, their efficiency and durability extension is what is targeted with this work.

A PEMFC converts hydrogen and oxygen into water, electricity and heat. It is made of successive layers and the core of a PEMFC is called the Membrane Electrode Assembly (MEA). It is composed of Gaz Diffusion Layers (GDL), Catalyst Layers (CL) and the electrolyte membrane. Around the MEA are two Bipolar Plates (BP) to feed the cell with gases, extract the water produced, remove heat, and connect the cell electrically and gaskets to avoid leakages. For real application, more power is required, hence these cells are assembled in series to build a stack giving it its name. The coolant, air or deionized water, flows in between head-to-head bipolar plates for temperature regulation.
The degradation of a PEMFC is commonly analysed through changes in its polarization curve, power output, or potential at nominal current. The model derived from this polarization curve typically accounts for macroscopic activation losses linked to electrochemical kinetics, ohmic losses associated with proton and electron conductivity in the membrane, GDL, and BP, as well as concentration losses related to gas transport through the GDL. However, the evolution of these losses cannot always be directly or precisely attributed to a single ageing phenomenon; instead, they serve as higher-level indicators.

As research on PEMFC ageing behaviour modelling continues to advance, with variations specific to each stack, new tools are enabling a deeper understanding of ageing phenomena, surpassing the limitations of insights provided by the polarization curve alone. By integrating this knowledge into ageing models, it becomes possible to enhance the prediction and the understanding of the state of health evolution in PEMFCs.

This work focuses on using the Distribution of Relaxation Times (DRT) on experimental electrochemical impedance spectroscopy (EIS). More and more studies are turning to EIS and DRT analysis for fuel cells [1], [2], [3]. The tools are used for different technologies from PEMFC to SOFC but mainly on single cells. Fewer studies on stacks can be found, and they are primarily focused on the impact of operating conditions on the EIS/DRT spectra rather than on applying this method to ageing data [4], [5].
This study presents one of the first attempts to using DRT on EIS measurements obtained from an industrial large-surface PEMFC short stack dedicated to heavy-duty transport application after an ageing campaign. Based on the methodology to assess the DRT results in a robust and

meaningful way proposed with a well-documented dataset, the newly produce data is analysed and gives promising results on using DRT to find ageing indicators that could later be used for ageing modelling of PEMFC. Moreover, the link between standard models using electric equivalent circuit and DRT is presented.

II. Degradation phenomena

The degradation phenomena can be described by component.

A. Membrane

The membrane allows protons to transfer from the anode to the cathode. A common material used is Nafion^{TM} that is composed of polyfluorosulfonic acid (PFSA) with hydrophobic chain of polytetrafluoroethylene (PTFE) to deal with water management and hydrophilic chain for the proton transport.
However, this structure can deteriorate due to O_2 permeation, which could be partially reduced in hydrogen peroxide H_2O_2 at the electrodes, ultimately degrading the polymer structure of the membrane. Additionally, the structure can be poisoned by multivalent cations (Fe^{3+}, Al^{3+}, etc.). The migration of platinum (Pt) in the membrane creating a Pt band also has a significant impact [6], [7].
Furthermore, the membrane is subjected to heavy mechanical stress due to the sealing requirements, which intensifies when the membrane becomes hydrated and expands, leading to increased mechanical and thermal strain.
All these phenomena can reduce the conductivity, create pinholes, and can be enhanced by other deterioration issues

B. Catalytic Layer (CL)

Electrochemical reactions occur at triple points in the CL. The triple points are active spots where the electrons, the protons and the gases (H_2/O_2) all come together around catalyst particles. To do this, Pt nanoparticles are applied on a layer of active carbon, which conducts the electrons. Meanwhile, this layer is surrounded by an ionomer to facilitate the diffusion of cations.
The main degradation factor is probably the alteration of Pt. First, one can observe that Pt particles tend to agglomerate in bigger structures, known as Ostwald ripening, that reduces the catalytic surface/volume ratio. The Pt oxidation and precipitation with H_2 into the membrane can create the Pt band explained in II.A. Moreover, the carbon layer can be oxidized by O_2 molecules, leading to more Pt structure detaching. The Pt can also be poisoned by CO, SO_2, NO, NH_3, etc., which reduces the Electrochemical Surface Area (ECSA), thereby reducing the efficiency as less species can react [6], [8].

C. Gas Diffusion Layer (GDL) and Bipolar Plates (BP)

The GDL is mainly impacted by carbon corrosion, which changes its microstructure and impacts its transport properties. When combined with the loss of PTFE, the GDL becomes less hydrophobic and the probability of water flooding increases [9].
The corrosion of bipolar plates increases their ohmic resistance, leading to a decline in the output voltage. This can also lead to membrane poisoning by cations, as described in II.A [10].

By understanding all these interdependent degradation phenomena, it becomes clear that the system is complex as they are all intricately linked, and one can cause chain reactions that will propagate through the different layers.

III. Analysing tools

EIS is a very useful tool to study the electrochemical properties of a system and decouple phenomena with different dynamics. By measuring the magnitude and phase response to a small amplitude voltage or current perturbation over a range of frequencies, an impedance spectrum is generated.
It can be expected that changes in key parameters such as the ohmic resistance or the capacitance of the PEMFC can be observed through the evolution of the impedance spectrum on the Nyquist plot.

Various analytical methods can then be used to interpret these changes and reveal the underlying degradation mechanisms.

A. Kramers-Kronig test

Before doing any data interpretation, one should always check the validity of the EIS measurements performed. To analyze the internal consistency of the data, one test proposed and commonly used is the Kramers-Kronig test also called KK-test. It verifies whether the obtained impedance spectrum is a representation of a linear, time-invariant and causal system and whether the data is consistent with these principles. The KK-test utilizes the real and imaginary part to compute their respective counterpart, and the quality of data is given relatively to the resulting residuals as given in (1) with $\Delta_{Re/Im}$ the deviation for the residuals, $Z_{Re/Im}$ the measured real or imaginary part, $\widehat{Z_{Re/Im}}$ the fitted real and imaginary parts and $|Z(\omega)|$, the module of the global impedance:

$$\begin{cases} \Delta_{Re}(\omega) = \dfrac{Z_{Re}(\omega) - \widehat{Z_{Re}}(\omega)}{|Z(\omega)|} \\ \Delta_{Im}(\omega) = \dfrac{Z_{Im}(\omega) - \widehat{Z_{Im}}(\omega)}{|Z(\omega)|} \end{cases} \quad (1)$$

A residuals deviation below 1%-2% is usually enough to validate the quality of the measurement.

B. Equivalent Circuit Modelling (ECM)

The ECM involves fitting the impedance spectrum using electrical components. The main components used are often well-known ones such resistors to represent the ohmic resistance and RC circuits for the reaction kinetics, but others are less common such as the infinite Warburg element for the mass transport loss at the cathode.
However, the limitations of the ECM method reside in the simplification of the system, the need for an *a priori* model that could evolve along the lifetime of the stack, the parameter determination that can be complicated due to the non-linearities and sometimes an equivalent circuit could have a good fitting whilst having no physical meaning. Moreover, the fitting process can be tedious and can be difficult to automate.
Hence, turning to a mathematical technique that can represent and interpret the Nyquist plot in a more meaningful way is appealing. This tool could also facilitate the fitting process as it will be demonstrated in this work.

C. Distribution of Relaxation Times (DRT)

The DRT method, a mathematical tool, offers deeper insights into the individual contribution of various phenomena to the impedance spectra. The DRT produces a distribution of time constants, $g(\tau)$, associated with an equivalent series of parallel RC circuits (2).

$$Z(\omega) = R_0 + R_{pol} \int_0^{\infty} \frac{g(\tau)}{1 + j\omega\tau} d\tau \quad (2)$$

Where R_0 is the ohmic resistance and R_{pol} is the polarization resistance. A time constant $\tau = RC$ is associated to each RC circuit. For discrete calculation, one can typically use an equally spaced logarithmic time constants giving (3).

$$Z(\omega) = R_0 + R_{pol} \sum_{k=1}^{N} \frac{g_k}{1 + j\omega\tau_k} \quad (3)$$

Heinzmann *et al.* [11] have shown in a highly controlled environment and on a single cell of 1 cm² that the resulting graph reveals distinct peaks associated with smaller scale phenomenon. For example, the peak at low frequency (~10Hz) is not present at low current density but appears and increases when current density increases too or when the partial pressure in oxygen decreases. This peak could be related to the increase of the gas diffusion contribution in the cathode GDL and CL to the impedance. The peak at medium frequency and its evolution with Relative Humidity leads to understanding that it is linked to the Oxygen Reduction Reaction (ORR), hence the charge transfer kinetics of the reaction. Finally, peaks at high frequency are more related to the proton transport in the CL.
For now, very few studies have been investigating finding the correlations between the working conditions and the physical phenomena at play in a short stack. This should be reminded as the interpretation of the peaks, because of the scale effect, is only possible under heavy hypotheses. Indeed, this does not consider the change in behavior for a bigger surface area that would be used in real-life applications as well as interactions between cells within a stack.
The tool used to calculate the DRT in this work is the pyDRTtool developed by F.Ciucci [12], [13], [14], [15], [16].

IV. Data and Experimental Set-up

A. Open source database

One database used for this study is collected from the IEEE PHM 2014 data challenge [17]. The 5-cell short stack FC2 was operated under rippled current at ± 10 % of the nominal current density within the frequency range of 0.05 Hz to 10 kHz. In particular, the EIS measurements performed under the different current densities 0.2, 0.45 and 0.7 A·cm^{-2} and different times across the duration of the ageing campaign at t = [0, 35, 182, 343, 515, 666, 830, 1016] h.

This database is mainly used as proof of concept for our methodology.

B. Test campaign

A second database has been collected on an up-to-date, industrial large-surface short stack designed for heavy-duty transportation. Then, comparing both results on both data, one could get an idea on the generalization of this method applied to short stacks of different number of cells, surface areas and power density. The EIS measurements performed also use a ± 10% of the nominal current AC perturbation. The frequency range goes from 0.05 Hz to 10 kHz. And the measurements have been performed throughout the ageing campaign timespan.

The test campaign has been designed to obtain the evolution of EIS. This first cycle was designed with stabilized steps at different current densities. This approach will help establish a baseline understanding of the ageing mechanisms and their progression under simplified conditions and enable the isolation and analysis of specific ageing phenomena or stress factors, such as thermal, electrochemical, or mechanical degradation. It has also enabled accelerated ageing, enabling the identification of long-term degradation trends within a shorter testing duration with thermal stress. Moreover, the constant-step cycles facilitate the calibration and validation of predictive ageing models which is the underlying objective for this study. In the process of understanding better the ageing behavior of DRT spectra of PEMFC for heavy-duty vehicles, complementary dynamic cycles are planned to be performed in later experimental campaigns.
Before and after each step, a polarization curve and EIS are performed. The operating conditions are always repeated for the characterization measurements to allow comparing results. The EIS measurements are also done at 4 different current densities to study the phenomena that happen across the current density range reachable by the PEMFC.

The ageing campaign is performed on a test bench from FCLAB depicted in Fig. 1 in Belfort, France. It allows controlling and regulating the pressures for the gases, the stoichiometries, the inlet temperature of the stack, the cooling system as well as measuring in real-time these parameters and the electrical data: current set on the electronic load and voltage across the short stack and per cell.

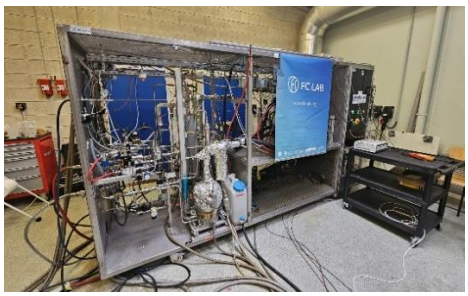


Fig. 1: Testbench used to run the ageing campaign on an industrial short stack dedicated to transportation application.

V. Results

A. Polarization curves

In Fig. 2 and Fig. 3, the evolution of polarization curves through time shows the impact of ageing, hence enforcing that these databases are suitable for our work.

For the campaign at FCLAB, the time is given in calendar time and not the operating time meaning it also considers the resting

time and interruptions in which one can observe some recovery processes. The stack has been operated for 61% of the total campaign time and stopped for 39% of the time.
The first curve at 334 h is done after an uninterrupted fixed working condition at medium current density. Then a second step was started at high current density, and an incident caused to work in dry conditions resulting in the curve at 421 h and a heavy degradation clearly visible in a bit more than 80 h. After one week and several characterizations, the polarization curve at 741 h was performed before starting the second step again. It shows that there is some recovery as the performances are higher than the previous curve. Finally, the curve at 796 h gives the end of step 2 and the beginning of step 3 at low current density and the last curve at 892 h is done at the end of this ageing campaign.

B. Validity of EIS on stack

The Kramers-Kronig test [18], [19], [20] was performed on the databases to evaluate the quality of the EIS measurements. A tolerance for the deviation of 2 % for the residuals was considered, and only the outliers were removed and replaced by the fitted value to keep the information. As stated before, the accuracy for the KK test is usually more restrictive but because a real system is used, more noise is necessarily induced, and defining this threshold therefore seems reasonable.

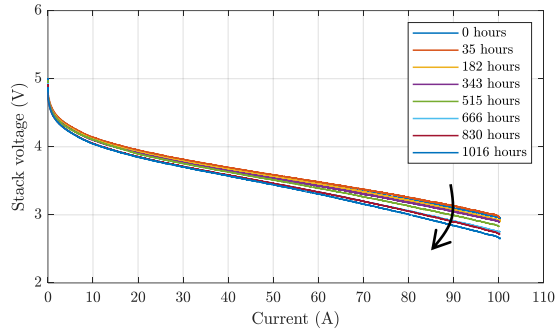


Fig. 2: Polarization Curves evolution with time of IEEE data.

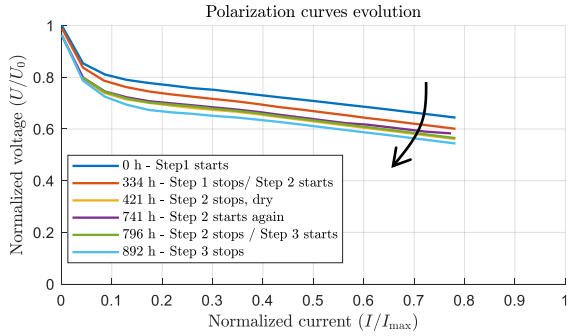


Fig. 3: Normalized polarization curves evolution with calendar time of original ageing campaign on an industrial stack (see text for detailed description of the various steps)

C. DRT on IEEE data

A sensitivity analysis of the DRT tool was already conducted on a previous study [21]. This tool proposes various settings depending on the approach and data under study and this preliminary work has allowed understanding which combination would be most suitable for this application. The Piecewise Linear discretization function with combined Re-Im data with an inductance contribution is used. The derivative used should of the 1st order and as the result is invariant to the regularization method, one can choose GCV, take 2500 samples and use the Bayesian Run.

In Fig. 4, the evolution of the DRT with time is presented. First, one can remark that there are not as many peaks as for the single cell as 5 peaks were found by Heinzmann *et al.* [11]. This is probably explainable in part because of the scale effect (×100) and the current density and also because not all phenomena are visible at all current levels. Secondly, there is a clear shift in amplitude and frequency with time as the darker blue line is at t = 0 h and lightest is at t = 1016 h. The dotted lines represent the confidence interval for this fitting; there is not much dispersion which is encouraging to extract figures related to ageing parameters in a later in-depth study.
In Fig 5, the result of fitting the EIS spectra with DRT is shown in the first graph, the experimental data are given in dotted lines. Below are the residuals for that fitting showing that whilst being still very acceptable the accuracy of the fitted model is better at higher frequencies where the stationarity hypothesis is easier to achieve.

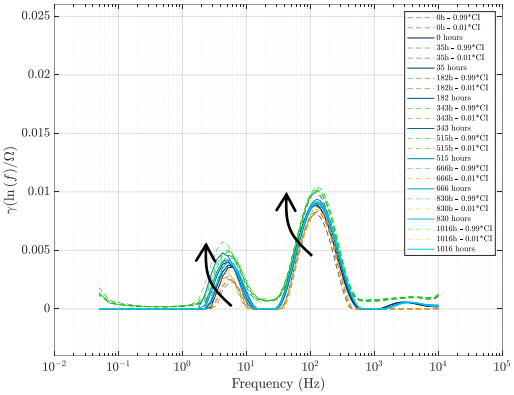


Fig. 4: DRT Maximum-A-Priori and Confidence Interval (CI) spectrum evolution with time at 0.2 A/cm² on IEEE data

At the frequencies peak 1 is located, it is likely related to the diffusion of gases based on results on single cells. However, the determination of the ageing phenomena that could be affected requires further investigations. Peak 2 should be related to the electrochemical surface, this conclusion is clearer when seeing the evolution of this peak with the current density which is not presented here.

D. DRT on industrial short-stack

For confidentiality reasons, some of the results presented in the next section are normalized.

In Fig. 6, compared to the IEEE dataset, the confidence interval in dotted lines is larger hence introducing more uncertainty on the interpretation. The confidence interval is only shown for the first curve at 0 h and the final one at 892 h to improve the readability of the results.

In Fig. 7, the solid lines represent the experimental data, and the dotted lines are the fitted ones. Here, the fitting is not as good as for the previous study, especially at lower frequencies. This could be explained by technology itself, the EIS measurement set up that differs and might be more sensible to noise at these frequencies. This could be improved by changing the parameters of DRT combined with a more elaborate experimental data treatment.

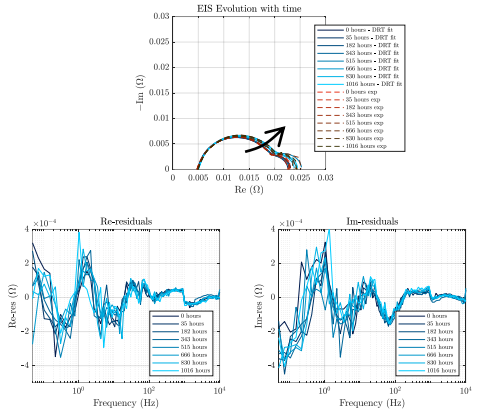


Fig 5: DRT Maximum-A-Priori spectrum evolution with time at 0.2 A/cm² on IEEE data.

As seen with the evolution of the polarization curves, the evolution of the DRT spectra is following the events from the ageing campaign. A shift in frequency is visible between the beginning of Step 2 at 334 h and the drying incident which was characterized at 421 h for both peaks. Then the amplitude increases consistently with time for peak 1. The recovery between 741 h and 796 h after working in controlled conditions at a high current density of 1.6 $A.cm^{-2}$ that helped rehydrate the short-stack membranes is also remarkable. Peak 2 amplitude on the contrary decreases after the drying incident but does not evolve much after that.

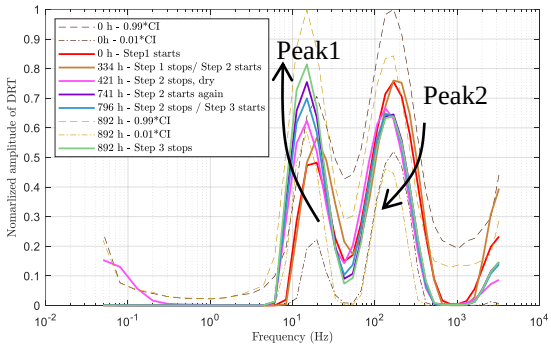


Fig. 6: DRT Maximum-A-Priori and Confidence Interval (CI) spectrum evolution with calendar time at low current density on industrial short-stack.

E. DRT and Equivalent Circuit Modelling

DRT, by showing clear peaks, allows assessing the structure of an Equivalent Circuit Model (ECM). Building on the knowledge given by the DRT spectrum, it shows only two main peaks should be enough to replicate the behavior demonstrated in the EIS plot using only two Constant Phase Element (CPE)//R circuits as shown in Fig 8. Here, since $n_2 = 1$, the second CPE behaves like an ideal capacitor.

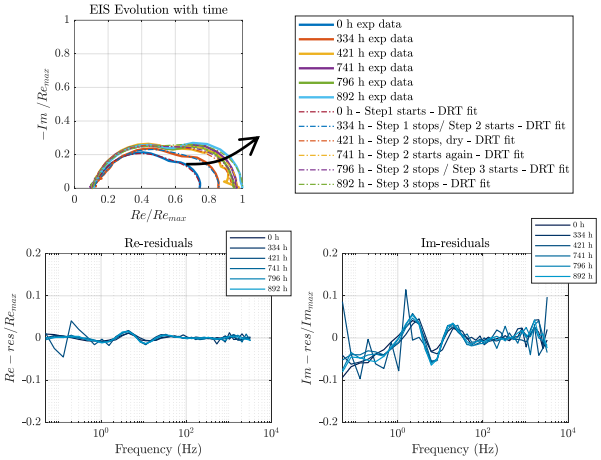


Fig. 7: DRT Maximum-A-Priori spectrum evolution with time at low current density on an industrial short-stack.

Then, defining the component is not sufficient and having the knowledge of the frequency of the max DRT amplitude helps having a first reliable approximation a lot quicker than it would be using the fitting algorithm implemented in softwares like ZView. Then, a given optimizer converges much faster to fit the experimental data understudied. The fitted in results are given in Fig 9.

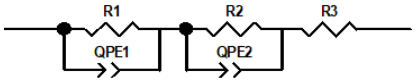


Fig 8: Equivalent Circuit model used to model the behavior of an industrial short stack based on the DRT analysis

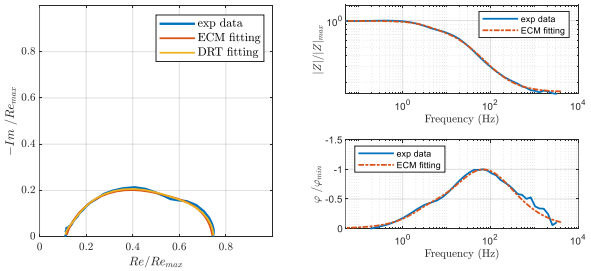


Fig 9: Comparison between fitting done with DRT and ECM

It is possible to compare the fitting obtained with the ECM and the DRT using the time constant of each equivalent circuit with equations given in (4). The frequencies are given in Table 1. There is a relative difference of 7.8 % for peak 1 and a relative difference of 5.6 % for peak 2.

$$f_{PEAKi} = R_i C_{i,eq} = Q_i^{\frac{1}{n_i}} R_i^{\frac{1-n_i}{n_i}} \text{ [22]} \quad (4)$$

EIS, Bode diagrams or DRT use the same raw data, then contain the same amount of information. But the DRT transform highlights the relevant dynamics and allows improving further and assessing the methodology for ECM.

Table 1: Comparison between the obtained frequencies using DRT and ECM

	$f_{PEAK1}(Hz)$	$f_{PEAK2}(Hz)$
DRT	19.65	168.1
ECM	21.2	158.6

VI. Disscussion and Conclusion

With the observable evolution of the DRT spectra with time, it has been shown that some ageing markers using DRT on transport dedicated PEMFC could be found. It has been shown that DRT can be used to improve the methodology for the ECM in defining the structure and the elements of the equivalent circuit and in optimizing the parameters to obtain a better fit.

The study of the evolution of DRT spectra with current density started on the IEEE data would also be very interesting to pursue on the new ageing campaign. Moreover, it has highlighted the need to conduct an in-depth analysis of the evolution of DRT with different working parameters to be able to identify more clearly the physical phenomena on the DRT graphs.

The generalization on the industrial large-surface short stack should be further studied but shows promising results as the tendency of evolution of DRT with time is coherent between the two studied short stacks. This comparison should also be enhanced by the current density analysis.

Finally, more ageing campaigns are planned to study the repeatability of the results on PEMFCs dedicated to transportation applications with more dynamic cycles.

Acknowledgment

Special thanks are addressed to Xavier François, Guillaume Barbette and Fabien Harel in their help to conduct the experimental campaign.

This work was supported by a grant from the French State, managed by the National Research Agency under the Investments for the Future program, reference ANR-21-ESRE-0033.
This work has also been supported by the EIPHI Graduate School (contract ANR-17-EURE-0002) and the Region Bourgogne Franche-Comté.

References

[1] H. Yuan, H. Dai, P. Ming, X. Wang, and X. Wei, ‘Quantitative analysis of internal polarization dynamics for polymer electrolyte membrane fuel cell by distribution of relaxation times of impedance’, *Appl. Energy*, vol. 303, p. 117640, 2021, doi: 10.1016/j.apenergy.2021.117640.

[2] H. Schichlein, A. C. Müller, M. Voigts, A. Krügel, and E. Ivers-Tiffée, ‘Deconvolution of electrochemical impedance spectra for the identification of electrode reaction mechanisms in solid oxide fuel cells’, *J. Appl. Electrochem.*, vol. 32, no. 8, pp. 875–882, 2002, doi: 10.1023/A:1020599525160.

[3] D. Zhu, Y. Yang, and T. Ma, ‘Evaluation the Resistance Growth of Aged Vehicular Proton Exchange Membrane Fuel Cell Stack by Distribution of Relaxation Times’, *Sustainability*, vol. 14, no. 9, p. 5677, Jan. 2022, doi: 10.3390/su14095677.

[4] J. Zuo, N. Y. Steiner, Z. Li, and D. Hissel, ‘Degradation root cause analysis of PEM fuel cells using distribution of relaxation times’, *Appl. Energy*, vol. 378, p. 124762, Jan. 2025, doi: 10.1016/j.apenergy.2024.124762.

[5] T. Reshetenko and A. Kulikovsky, ‘Understanding the distribution of relaxation times of a low–Pt PEM fuel cell’, *Electrochimica Acta*, vol. 391, p. 138954, Sep. 2021, doi: 10.1016/j.electacta.2021.138954.

[6] F. Bruijn, V. A. Dam, and G. Janssen, ‘Review: Durability and Degradation Issues of PEM Fuel Cell Components’, *Fuel Cells*, vol. 8, pp. 3–22, Feb. 2008, doi: 10.1002/fuce.200700053.

[7] W. Touil, Z. Li, R. Outbib, D. Hissel, and S. Jemei, ‘Control oriented modeling of integrated catalyst and membrane degradation in PEM fuel cells’, in *2024 IEEE Transportation Electrification Conference and Expo (ITEC)*, Jun. 2024, pp. 1–7. doi: 10.1109/ITEC60657.2024.10598861.

[8] R. E. Rosli *et al.*, ‘A review of high-temperature proton exchange membrane fuel cell (HT-PEMFC) system’, *Int. J. Hydrog. Energy*, vol. 42, no. 14, pp. 9293–9314, Apr. 2017, doi: 10.1016/j.ijhydene.2016.06.211.

[9] K.-Y. Song and H.-T. Kim, ‘Effect of air purging and dry operation on durability of PEMFC under freeze/thaw cycles’, *Int. J. Hydrog. Energy*, vol. 36, no. 19, pp. 12417–12426, Sep. 2011, doi: 10.1016/j.ijhydene.2011.06.095.

[10] M. Kumagai, S.-T. Myung, S. Kuwata, R. Asaishi, and H. Yashiro, ‘Corrosion behavior of austenitic stainless steels as a function of pH for use as bipolar plates in polymer electrolyte membrane fuel cells’, *Electrochimica Acta*, vol. 53, no. 12, pp. 4205–4212, May 2008, doi: 10.1016/j.electacta.2007.12.078.

[11] M. Heinzmann, A. Weber, and E. Ivers-Tiffée, ‘Advanced impedance study of polymer electrolyte membrane single cells by means of distribution of relaxation times’, *J. Power Sources*, vol. 402, pp. 24–33, Oct. 2018, doi: 10.1016/j.jpowsour.2018.09.004.

[12] M. B. Effat and F. Ciucci, ‘Bayesian and Hierarchical Bayesian Based Regularization for Deconvolving the Distribution of Relaxation Times from Electrochemical Impedance Spectroscopy Data’, *Electrochimica Acta*, vol. 247, pp. 1117–1129, Sep. 2017, doi: 10.1016/j.electacta.2017.07.050.

[13] T. H. Wan, M. Saccoccio, C. Chen, and F. Ciucci, ‘Influence of the Discretization Methods on the Distribution of Relaxation Times Deconvolution: Implementing Radial Basis Functions with DRTtools’, *Electrochimica Acta*, vol. 184, pp. 483–499, Dec. 2015, doi: 10.1016/j.electacta.2015.09.097.

[14] F. Ciucci, *pyDRTtool*. (2025). Python. [Online]. Available: https://github.com/ciuccislab/pyDRTtools

[15] A. Maradesa, B. Py, T. H. Wan, M. B. Effat, and F. Ciucci, ‘Selecting the Regularization Parameter in the Distribution of Relaxation Times’, *J. Electrochem. Soc.*, vol. 170, no. 3, p. 030502, Mar. 2023, doi: 10.1149/1945-7111/acbca4.

[16] F. Ciucci and C. Chen, ‘Analysis of Electrochemical Impedance Spectroscopy Data Using the Distribution of Relaxation Times: A Bayesian and Hierarchical Bayesian Approach’, *Electrochimica Acta*, vol. 167, pp. 439–454, Jun. 2015, doi: 10.1016/j.electacta.2015.03.123.

[17] E. Pahon, M.-C. Péra, D. Bouquain, and D. Hissel, ‘Impact of current ripples on the durability of proton exchange membrane fuel cells based on two ageing datasets’, *Data Brief*, vol. 45, p. 108601, Dec. 2022, doi: 10.1016/j.dib.2022.108601.

[18] M. Schönleber, D. Klotz, and E. Ivers-Tiffée, ‘A Method for Improving the Robustness of linear Kramers-Kronig Validity Tests’, *Electrochimica Acta*, vol. 131, pp. 20–27, Jun. 2014, doi: 10.1016/j.electacta.2014.01.034.

[19] B. A. Boukamp, ‘A Linear Kronig-Kramers Transform Test for Immittance Data Validation’, *J. Electrochem. Soc.*, vol. 142, no. 6, p. 1885, Jun. 1995, doi: 10.1149/1.2044210.

[20] A. Weber, *Lin-KK tool*. (2015). [Online]. Available: https://www.iam.kit.edu/et/english/Lin-KK.php

[21] L. Turpin, Q. Cacciuttolo, B. Xu, Z. Zheng, and M.-C. Péra, ‘Ageing phenomena identification of PEMFC using the DRT tool’, in *6ème Symposium de Génie Électrique*, Toulouse, France: SGE-Conf, Jul. 2025. Accessed: Apr. 15, 2026. [Online]. Available: https://hal.science/hal-05317401

[22] J. Bisquert and E. H. Balaguera, ‘Brief Guide to Transformation of Constant Phase Element Impedance to Equivalent Capacitor or Inductor’, *J. Phys. Chem. Lett.*, vol. 16, no. 23, pp. 5779–5783, Jun. 2025, doi: 10.1021/acs.jpclett.5c01131.